

Infrared Spectroscopic Study of the Binary Blends of Sodium and Zinc Salt Ionomers Produced from Poly(ethylene-*co*-methacrylic acid)

Shoichi Kutsumizu*

Instrumental Analysis Center, Gifu University, 1-1 Yanagido, Gifu 501-1193, Japan

Hisaaki Hara and Hitoshi Tachino

Technical Center, Du Pont-Mitsui Polychemicals Company, Limited, 6 Chigusa-kaigan, Ichihara, Chiba 299-0108, Japan

Katsuomi Shimabayashi and Shinichi Yano

Department of Chemistry, Faculty of Engineering, Gifu University, 1-1 Yanagido, Gifu 501-1193, Japan

Received April 12, 1999; Revised Manuscript Received June 28, 1999

ABSTRACT: Infrared (IR) and far-infrared studies were performed for the binary blends of sodium and zinc salt ionomers of poly(ethylene-*co*-methacrylic acid) (EMAA), which are known to show a dramatic improvement of small strain moduli (e.g., stiffness) compared with the two component salts. The IR spectra of the blends showed a new asymmetric carboxylate stretching band at 1569 cm^{-1} , which is assigned to carboxylate groups bridging sodium and zinc cations. When temperature was raised, the bandwidth began to increase at around 310 K, just below a transition temperature ($T_i = \text{ca. } 325\text{ K}$) observed by DSC and far below the melting of polyethylene crystalline region ($T_m = \text{ca. } 360\text{ K}$); this increase was almost linear with temperature and continued to 403 K above T_m , reflecting the increased distribution of the states of the bridging mode with temperature. These results are explained by a structural transition of ionic aggregates at T_i in EMAA ionomers, which was proposed in our previous publications.

Introduction

Ionomers are ion-containing polymers containing typically hydrophobic backbones and a relatively small amount of ionic groups such as carboxylic, sulfonic, and phosphoric acids, etc., where the acid groups are partially or fully neutralized with metal cations. Extensive research on the microstructure of ionomers has been done over the past three decades, and it has been shown that ionic groups tend to form microphase-separated ionic aggregates, called multiplets, ionic clusters, or ionic domains, which are crucial for the unique physicochemical properties of ionomers.^{1–4} Although many types of ionomers have been developed to date, ethylene ionomers produced from poly(ethylene-*co*-methacrylic acid) (EMAA) and perfluorinated ionomers known as Nafion and Flemion are commercially very important because of their useful applications.

The technology of blending two ethylene ionomers neutralized with different metal cations has been practiced for years in some industrial applications⁵ because such ionomer blends intensify and/or modify greatly their characteristic properties such as stiffness, yield strength, and moisture absorption. Therefore, it is worthwhile clarifying the mechanism of the effect of blending two metal cation ionomers on their microstructure and properties. Until recently, however, there were no systematic studies that focus on this interesting phenomenon, and this was one reason we initiated our studies on blending two metal cation ionomers. In our previous studies,⁶ we examined binary blends selected from Li, Na, Mg, Cu(II), and Zn(II) salts of EMAA, by use of stiffness, tensile strength, dynamic mechanical measurements, differential scanning calorimetry (DSC), and infrared (IR) spectroscopy. These studies revealed

that the binary blends unexpectedly give higher small-strain moduli such as stiffness and yield stress, if cations are selected from different metal groups such as alkali, alkaline-earth, and transition metals. In the binary blends of sodium and zinc salt ionomers, the DSC and IR studies suggest the formation of a new structure in the ionic aggregates, which consists of a conjugated binary metal salts containing sodium and zinc carboxylates, and unneutralized carboxylic acid, and this formation is considered to be responsible for the enhancement of small-strain moduli.

The DSC thermogram for the sodium–zinc mixed ionomers shows two endothermic peaks near 325 and 360 K on heating after aging at room temperature for more than several days. This result is essentially identical with that for other EMAA ionomers neutralized with single cations, and the higher temperature peak corresponds to the melting of polyethylene crystalline region (T_m), and on the basis of our proposed model,⁷ the lower one is assigned to a transition associated with ionic aggregate regions (T_i). Unfortunately, the assignment of the T_i transition is still a subject of debate,⁸ but the nature of the T_i transition is an important problem because the viscoelastic properties of EMAA ionomers drastically change at T_i and, moreover, some mechanical properties such as stiffness at room temperature are strongly correlated with the value of transition enthalpy at T_i .⁹

IR or far-IR spectroscopy is a useful technique to investigate the local environments of ionic groups in ionomers,¹⁰ and in EMAA ionomers, the bands due to the asymmetric stretching vibrations of carboxylate groups ($\nu_{\text{as}}(\text{COO}^-)$) in the region $1650\text{--}1500\text{ cm}^{-1}$ can be employed for this purpose.^{11–18} In the region below 400 cm^{-1} , the bands due to cation–oxygen vibration in the cation–carboxylate complexes are also interesting because of their sensitivity to ionic aggregations.^{19–21}

* To whom correspondence should be addressed. E-mail: kutsu@cc.gifu-u.ac.jp.

The present paper reports IR and far-IR spectroscopic studies of the sodium–zinc mixed ionomers mentioned above, especially concentrating on a new $\nu_{\text{as}}(\text{COO}^-)$ band at 1569 cm^{-1} , which is absent for individual ionomers and is therefore assigned to carboxylate groups bridging sodium and zinc cations. Temperature-dependent IR studies were carried out over a temperature range from room temperature to $130\text{ }^{\circ}\text{C}$ (403 K). The results demonstrate that the transition at T_i changes the dynamical states of the bridging carboxylate groups in the ionic aggregates, which supports the ionic aggregate transition model of EMAA ionomers.⁷ Selected preliminary results have been presented.²²

Experimental Section

Materials. The precursor EMAA resin is a random copolymer of ethylene and methacrylic acid (MAA), and the MAA content is 5.4 mol %. Sodium–zinc mixed ionomers of EMAA were prepared according to the method reported previously.⁶ In the present paper, the samples are denoted as EMAA–0.3Na/EMAA–0.6Zn (x/y w/w), where 0.3Na and 0.6Zn indicate that the neutralizations with sodium and zinc are 30% and 60%, respectively, and x/y is the blend ratio of two cation ionomers, which is equal to the molar ratio of sodium to zinc ions in the blend. DSC experiments at a rate of 10 K/min for EMAA–0.3Na/EMAA–0.6Zn (75/25 w/w) showed T_i at 326 K (on the first heating for an aged compression-molded sample) and T_m at 364 K .⁶

Measurements. The $10\text{--}30\text{-}\mu\text{m}$ -thick films for IR analysis were prepared by compression-molding at 5 MPa and 453 K , and stored at room temperature in a vacuum desiccator for 3–4 weeks. IR spectra at elevated temperatures were measured for EMAA–0.3Na/EMAA–0.6Zn (75/25 w/w) using a Perkin-Elmer 1640 FT-IR spectrometer, equipped by a heated cell (S.T. Japan, type 0019–201) and a temperature controller (S.T. Japan, type 0019–200). Each trace represents the average of 64 scans at a resolution of 4 cm^{-1} . Digital encoding of the spectral data was carried out at 2 cm^{-1} intervals, transferred into an EPSON PC-486GR personal computer for further calculations described below: The baseline of each spectrum was assumed to be a line through two minimum points, one in the region $500\text{--}1700\text{ cm}^{-1}$ and the other in the region $1700\text{--}2000\text{ cm}^{-1}$. After the baseline subtraction, the spectrum was resolved in the region $1522\text{--}1796\text{ cm}^{-1}$ with a modified version of the curve-fitting program originally developed by Minami²³ as a BASIC program. The program includes Davidon-Fletcher-Powell optimization routine,²⁴ and each absorption peak was given by a Gauss-Lorentz function^{25,26} as

$$F(\nu) = H \exp[-(\ln 2)((\nu_0 - \nu)/W_1)^2] / (1 + ((\nu_0 - \nu)/W_2)^2) \quad (1)$$

where ν_0 (peak frequency), H (peak intensity at ν_0), W_1 (half-bandwidth at half-maximum in Gaussian component), and W_2 (half-bandwidth at half-maximum in Lorentzian component) are adjustable parameters.

Far-infrared (far-IR) spectra were measured with a Perkin-Elmer system 2000 FT-IR spectrometer at room temperature, using a homemade sample holder to eliminate the influence of water vibrations. The film thickness was about $300\text{ }\mu\text{m}$, and 1024 scans at a resolution of 4 cm^{-1} were signal averaged.

X-ray scattering measurements were carried out using about 0.5-mm -thick sheets with a Mac Science X-ray diffraction system MXP³ at the Instrument Center, Institute for Molecular Science, Okazaki, Japan. The instrument was operated with a copper target at a 50-kV accelerating potential and 40-mA emission current. The $\text{Cu K}\alpha$ radiation ($\lambda = 1.54050\text{ }\text{\AA}$) was selected with a graphite monochromator. Samples were scanned at $2.0^\circ\text{ min}^{-1}$ at room temperature.

Results and Discussion

X-ray Scattering. Figure 1 shows the X-ray scattering patterns in the low-angle region for EMAA–0.3Na, EMAA–0.6Zn, and the blends. All samples show a

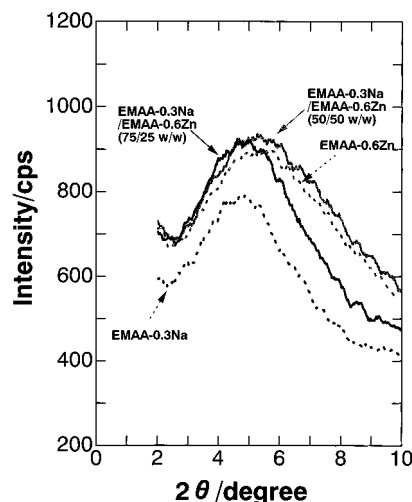


Figure 1. X-ray scattering patterns in the small-angle region for binary blends of EMAA–0.3Na and EMAA–0.6Zn.

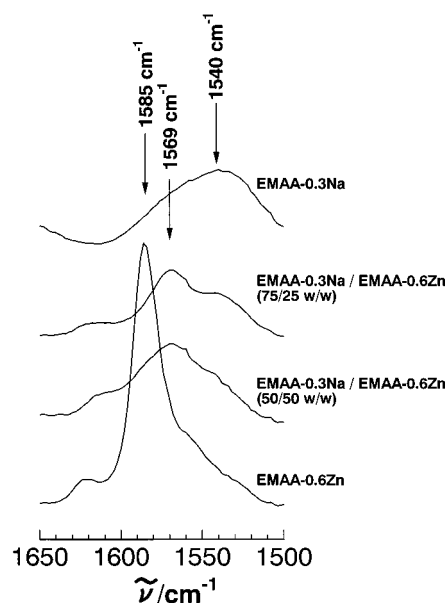


Figure 2. Infrared spectra in the carboxylate asymmetric stretching region for binary blends of EMAA–0.3Na and EMAA–0.6Zn at room temperature. Each spectrum is normalized with respect to the absorbance of the 1467 cm^{-1} band because it is scarcely affected with neutralization.¹⁴

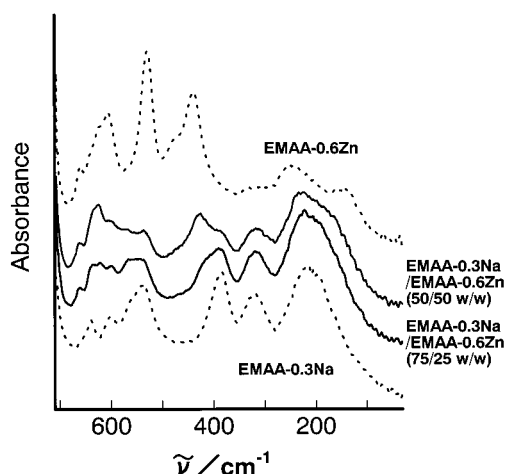
single broad peak at around $2\theta = 5^\circ$. This peak is called an ionic peak and the origin is the aggregation of ionic groups such as $-\text{COONa}$ and $-\text{COOZn}_{1/2}$ in these ionomers.^{3,4} Interestingly, EMAA–0.3Na/EMAA–0.6Zn (75/25 w/w) shows a sharper peak than the other three, and that peak is much larger than the linear combination of two ionic peaks of EMAA–0.3Na and EMAA–0.6Zn with a ratio of 75/25. These results suggest that in EMAA–0.3Na/EMAA–0.6Zn (75/25 w/w), sodium and zinc cations are mixed at the molecular level to form ionic aggregates and that the ionic aggregation is higher than expected for a simple mixing of EMAA–0.3Na and EMAA–0.6Zn.

IR Spectra and Peak Assignment. Figure 2 shows the IR spectra of EMAA–0.3Na/EMAA–0.6Zn blends in the region from 1500 to 1650 cm^{-1} , which is associated with the asymmetric stretching vibration region of carboxylate group ($\nu_{\text{as}}(\text{COO}^-)$). The $\nu_{\text{as}}(\text{COO}^-)$ bands of EMAA–0.6Zn consist of a strong peak at 1585 cm^{-1} , a small peak at 1620 cm^{-1} , and two weak shoulder

Table 1. Tentative Band Assignments for EMAA–0.3Na/EMAA–0.6Zn (75/25 w/w)^a

peak position, cm ⁻¹		assignment (abbreviation)
293 K	403 K	
n.o.	1750	C=O str vibr of free COOH ($\nu(\text{C=O})_{\text{free}}$)
1699	1702	C=O str vibr of H-bonded COOH ($\nu(\text{C=O})_{\text{dimer}}$)
1616	1611	COO ⁻ asym str vibr ($\nu_{\text{as}}(\text{COO}^-)$)
1569	1564	COO ⁻ asym str vibr ($\nu_{\text{as}}(\text{COO}^-)$)
1538 (sh)	1546	COO ⁻ asym str vibr ($\nu_{\text{as}}(\text{COO}^-)$)
1467	1464	CH ₂ bend vibr from both cryst and amorphous regions ($\delta(\text{CH}_2)$)
1407	1403	C–O str vibr of H-bonded COOH ($\nu(\text{C–O})_{\text{dimer}}$) coupled with O–H in-plane bend + COO ⁻ sym str vibr ($\nu_{\text{s}}(\text{COO}^-)$)
1378	1379	CH ₃ sym def ($\delta_{\text{s}}(\text{CH}_3)$)
~1370 (sh)	1367	CH ₂ wag vibr from amorphous regions ($w(\text{CH}_2)$)
~1300 (sh)	~1300 (sh)	CH ₂ twist vibr from amorphous regions ($t(\text{CH}_2)$) + C–O str vibr of free COOH ($\nu(\text{C–O})_{\text{free}}$)
1260	1258	C–O str vibr of H-bonded COOH ($\nu(\text{C–O})_{\text{dimer}}$) coupled with O–H in-plane bend
~1180 (sh)	~1190 (sh)	C–O str vibr of H-bonded COOH ($\nu(\text{C–O})_{\text{dimer}}$) coupled with O–H in-plane bend?
1096	1094	C–C skeletal str vibr from amorphous regions
940 (br)	930 (br)	out-of-plane bend of H-bonded OH ($\gamma_{\text{O–H}}$)
730 (sh)	n.o.	CH ₂ rock vibr from cryst regions ($r(\text{CH}_2)$)
720	720	CH ₂ rock vibr from both cryst and amorphous regions ($r(\text{CH}_2)$)

^a Key: n.o., not observed; sh, shoulder; br, broad; str, stretching; asym, asymmetric; sym, symmetric; bend, bending; cryst, crystalline; def, deformation; wag, wagging; twist, twisting; rock, rocking.

**Figure 3.** Far-infrared spectra of binary blends of EMAA–0.3Na and EMAA–0.6Zn at room temperature. Each spectrum is normalized to the same film thickness of 300 μm .

peaks at 1560 and 1535 cm^{-1} , as reported by Coleman et al.,¹⁵ while those of EMAA–0.3Na show a very broad peak centered at 1540 cm^{-1} , with a tail in its high wavenumber side. In two EMAA–0.3Na/EMAA–0.6Zn blends, the contour of the $\nu_{\text{as}}(\text{COO}^-)$ bands is very different from the band shapes of the two neat ionomers; the $\nu_{\text{as}}(\text{COO}^-)$ bands have a peak at 1569 cm^{-1} with two shoulder peaks at 1538 and 1616 cm^{-1} . These differences reflect changes in the local environment of the neutralizing cations with the blending, indicating that EMAA–0.3Na/EMAA–0.6Zn (75/25 w/w) forms a new structure in the ionic aggregates; the new structure is proposed to consist of a conjugated binary metal salts containing sodium and zinc carboxylates and unneutralized carboxylic acid, similar to solvated sodium zinc acetate, $\text{Zn}(\text{CH}_3\text{COO})_2 \cdot 2\text{Na}(\text{CH}_3\text{COO}) \cdot 4\text{CH}_3\text{COOH}$.²⁷ This conclusion was supported by other observations that were fully discussed in ref 6:

(1) Small-strain moduli such as stiffness and yield stress have shown a maximum around 75 wt % of EMAA–0.3Na, and their values are much higher than those of the neat ionomers. This effect of blending two cation ionomers is explained by some drastic structural changes in the ionic aggregates, because the structure and cohesiveness of ionic aggregates strongly influence small-strain moduli.

(2) Dynamic mechanical measurements have shown that 50/50 w/w mixing of EMAA–0.3Na and EMAA–0.6Zn moves a $\tan \delta$ peak of the α relaxation to a temperature 10 K higher than that of EMAA–0.3Na, whereas EMAA–0.6Zn shows no α peak. The α relaxation reflects the motion of polymer chains attached to the ionic aggregate region, and the higher-temperature shift implies a promoted microphase separation of ionic aggregate region from the amorphous region in the 50/50 w/w blend.

(3) The moisture absorption at 50% relative humidity was greatly reduced in the 50/50 w/w blend, compared with that of EMAA–0.3Na, almost to the level of that of EMAA–0.6Zn. This reduction allows us speculation that the nature of ionic aggregates is changed by blending two cation ionomers.

The tentative assignments of main IR peaks for EMAA–0.3Na/EMAA–0.6Zn (75/25 w/w) are summarized in Table 1.

Far-IR Spectra. Figure 3 shows the far-IR spectra of EMAA–0.3Na/EMAA–0.6Zn blends in the region 30–710 cm^{-1} . EMAA–0.3Na shows a broad band at 216 cm^{-1} , which is assigned to the Na–O vibration of the Na⁺-carboxylate complex.¹⁹ With the addition of 25 w % EMAA–0.6Zn, the corresponding peak is seen at 221 cm^{-1} with almost the same intensity. With a further increase in the content of EMAA–0.6Zn, in EMAA–0.3Na/EMAA–0.6Zn (50/50 w/w), this peak begins to split into two peaks, a peak at 227 cm^{-1} and a shoulder peak at around 160 cm^{-1} , and into two well-defined peaks at 245 and 142 cm^{-1} in EMAA–0.6Zn. In our previous paper,²¹ the 245 and 142 cm^{-1} bands were assigned to the vibrational modes of Zn(II) ions incorporated in the ionic aggregates and of isolated Zn(II) ions, respectively. Therefore, the shoulder peak at around 160 cm^{-1} is also related to the presence of isolated cations in EMAA–0.3Na/EMAA–0.6Zn (50/50 w/w).

It is useful to plot the frequency (ν) of the cation–O vibration vs the inverse square root of the cation mass ($1/\sqrt{M}$), where M is the cation mass. Mattera and Risen²⁰ reported that in poly(styrene sulfonic acid) ionomers the plots of ν vs $1/\sqrt{M}$ are almost linear for a given group such as alkali or alkaline-earth metal, and that the slope of the divalent cation salts is 1.6 times larger than that for the monovalent cation salts. The

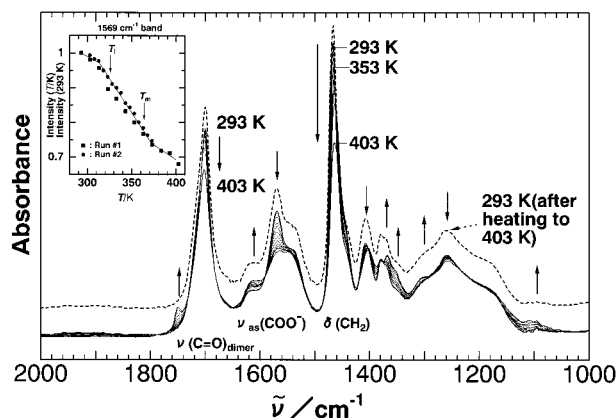


Figure 4. Infrared spectra in the region 1000–2000 cm^{-1} of EMAA–0.3Na/EMAA–0.6Zn (75/25 w/w), taken at 10 K intervals from 293 to 403 K. Arrows indicate the variation in peak intensity with temperature. Inset shows the peak intensity of the 1569 cm^{-1} band as a function of temperature, where the solid lines are a guide for the eye.

slope is regarded as a measure of the force constant (k) of the cation–O vibration because $\nu = \sqrt{(k/M)}$. The same plots were made for EMAA–0.3Na/EMAA–0.6Zn blends, where the cation mass of the two blends was assumed to be a linear combination of two cation masses with the blending ratio. The result showed that the value of k is on the order of EMAA–0.3Na (1.0) < EMAA–0.3Na/EMAA–0.6Zn (75/25 w/w) (1.5) < EMAA–0.3Na/EMAA–0.6Zn (50/50 w/w) (2.1) < EMAA–0.6Zn (3.7), where the values relative to that of EMAA–0.3Na are shown in parentheses. Hence, the value of k increases almost linearly with the content of EMAA–0.6Zn.

Another thing to note is in the region near 500 cm^{-1} . A strong band is seen at 529 cm^{-1} in EMAA–0.6Zn, and EMAA–0.3Na shows a weak band at 536 cm^{-1} . In the two blends, however, the corresponding peak is significantly suppressed. The assignment of these bands is not completely clear, because the band at $\sim 530 \text{ cm}^{-1}$ possibly contains a few vibrational modes. Stoilova et al.²⁸ examined IR spectra of several metal(II) acetate hydrates and assigned the peak observed at $\sim 530 \text{ cm}^{-1}$ to out-of-plane COO^- bending vibrations. They pointed out that this peak is absent if the acetate ligand is bridged or substantially reduced for bidentate acetate ligands. Their criterion and our observations on EMAA–0.3Na/EMAA–0.6Zn blends supported our conclusion that some of the carboxylate groups are in the bridging modes such as $\text{Na}^+ - \text{OCO}^- - \text{Zn}^{2+}$.

IR Spectra at Elevated Temperatures. Figure 4 shows the IR spectra in the 1000–2000 cm^{-1} region, taken at 10 K intervals from 293 to 403 K. First, a strong peak at 1467 cm^{-1} decreases in intensity and broadens with increasing temperature. This decrease is notable above about 353 K. The 1467 cm^{-1} peak is assigned to the CH_2 bending vibrations ($\delta(\text{CH}_2)$) of ethylene backbones in both crystalline and amorphous regions,^{10,11} and therefore, the observed decrease is clearly due to the melting of polyethylene crystalline regions whose melting temperature (T_m) determined by DSC is 364 K.

Second, the C=O stretching ($\nu(\text{C=O})_{\text{dimer}}$) band at 1699 cm^{-1} ¹² decreases as temperature is raised, notably above T_m . This decrease is accompanied by the appearance of a new band at 1750 cm^{-1} , which grows with increasing temperature. An isosbestic point is seen at 1731 cm^{-1} . The 1699 and 1750 cm^{-1} bands come from

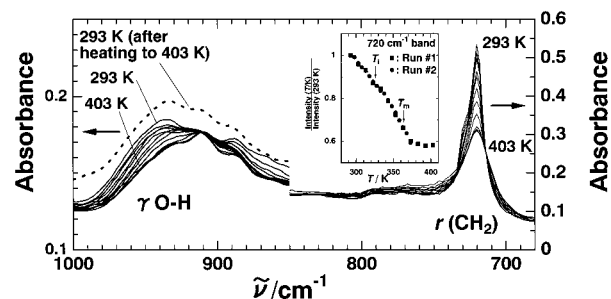


Figure 5. Infrared spectra in the region 680–1000 cm^{-1} of EMAA–0.3Na/EMAA–0.6Zn (75/25 w/w), taken at 10 K intervals from 293 to 403 K. Inset shows the peak intensity of the 720 cm^{-1} band as a function of temperature.

hydrogen-bonded COOH dimers and free COOH monomers, respectively, and the observed spectral change indicates the dissociation of hydrogen-bonded COOH dimers into the monomers with increasing temperature.

Third, the most interesting change is seen in the region of 1500–1650 cm^{-1} , where three overlapping bands at 1616, 1569, and 1538 cm^{-1} are observed. When the temperature is raised, the 1569 cm^{-1} band decreases and the 1616 cm^{-1} band slightly increases. Since these three bands are all assigned to COO^- asymmetric stretching vibrations ($\nu_{\text{as}}(\text{COO}^-)$), the observed spectral changes may imply changes in the local environment of the neutralizing cations with temperature. In the inset, the peak intensity of the 1569 cm^{-1} band is plotted as a function of temperature. The slope of the intensity–temperature curve is initially small and at around T_i ($=326 \text{ K}$) becomes steeper and at around T_m again becomes small. Therefore, the 1569 cm^{-1} band changes at two characteristic temperatures of this ionomer, T_i and T_m . As mentioned above, T_m is the melting point of the polyethylene crystalline region. The assignment of T_i is still subject to debate, but T_i is probably the softening temperature of the ionic aggregate region. The fact that the rapid decrease starts at around T_i supports that the transition at T_i is associated with some changes inside the ionic aggregate region. Finally, it is noted that the spectrum, including the $\nu_{\text{as}}(\text{COO}^-)$ region, completely reverted to the original one when the sample was cooled to 293 K after this experiment. This important result will be discussed later in detail.

The temperature variation of the region 680–1000 cm^{-1} is shown in Figure 5. The broad band centered at 940 cm^{-1} at 293 K is assigned to the out-of-plane bending vibrations of hydrogen-bonded OH ($\gamma_{\text{O-H}}$).¹¹ As temperature is increased, this band diminishes and moves to a little bit lower wavenumber, and at 403 K, it is only seen as a weak shoulder at 930 cm^{-1} , indicating that the hydrogen bonding is weakened with increasing temperature. The dotted curve is the spectrum after cooling from 403 to 293 K and waiting for 2 h. This spectrum is identical with the original spectrum before heating. Therefore, it is concluded that the hydrogen bonding formed by COOH groups is almost perfectly restored at 293 K after the heating and cooling process.

In Figure 5, another prominent change with temperature is seen at around 720 cm^{-1} ; as the temperature is raised, the 720 cm^{-1} peak decreases, and concurrently, the shoulder peak at 730 cm^{-1} also decreases and virtually disappears above T_m . As is well-known, both 720 and 730 cm^{-1} peaks are associated with the CH_2 rocking vibrations ($r(\text{CH}_2)$) of polyethylene

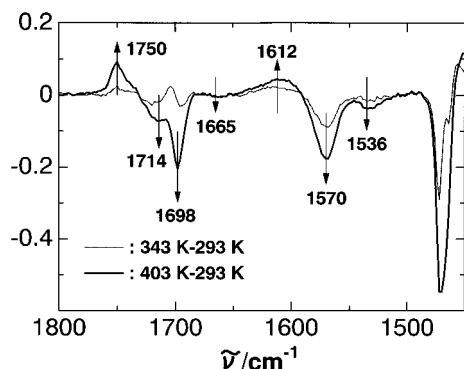


Figure 6. Difference spectra obtained by (a) subtracting the spectrum at 293 K from the spectrum at 343 K (gray) and (b) subtracting the spectrum at 293 K from the spectrum at 403 K (black), where peak maxima and minima indicate, respectively, increasing and decreasing in peak intensity of the bands at designated wavenumbers with increasing temperature.

chains.^{11,29} The 730 cm^{-1} shoulder peak is from the crystalline region and is assigned to the in-phase vibrations for two chains in the unit cell. The 720 cm^{-1} peak, on the other hand, contains both crystalline and amorphous components; the crystalline component is assigned to the out-of-phase CH_2 rocking vibrations for two chains in the unit cell, and the amorphous one arises from the CH_2 rocking vibrations of chain segments in the trans conformation. As shown in the inset, plotting the peak intensity of the 720 cm^{-1} band vs temperature can provide us with some information on the state of polyethylene chains in this ionomer. It is very interesting that the decrease in the intensity starts around room temperature, far below T_m . The slope of the decrease becomes slightly steeper at around 340 K, a little bit higher than T_i , but levels off at around 370 K over T_m . It is clear that such a decrease corresponds to the melting process of the polyethylene crystalline region, and it may be said that the potential melting starts to occur around room temperature.

Band Resolution of the IR Spectra. The present paper concentrates on the changes in the local environments of the Na/Zn carboxylate groups with temperature, and as clearly shown in Figure 4, the asymmetric carboxylate stretching ($\nu_{\text{as}}(\text{COO}^-)$) band at 1569 cm^{-1} , attributable to carboxylate groups bridging sodium and zinc cations, was changed with temperature. In other words, the 1569 cm^{-1} band can act as a probe monitoring the dynamics in the ionic aggregates with increasing temperature. To get more quantitative information, it is necessary to resolve the three overlapping bands in the region 1650–1500 cm^{-1} . Since the band at 1616 cm^{-1} seems to be severely overlapped by two bands at 1699 and 1569 cm^{-1} , it is necessary to include the region of 1800–1650 cm^{-1} for the calculation. Strictly speaking, the same situation may be considered with the 1538 cm^{-1} band because this band is close to the strong band at 1467 cm^{-1} , but taking the region below 1500 cm^{-1} into consideration would make the calculation virtually impossible. So, we treated the spectral pattern in the region 1800–1500 cm^{-1} .

Figure 6 shows the difference spectra obtained by subtracting the spectrum at 293 K from the spectrum at 343 and 403 K, respectively, where peak maximum and minimum indicate, respectively, increasing and decreasing peak intensity with increasing temperature at designated wavenumbers. In the region 1800–1500 cm^{-1} , there are observed seven peaks, two maxima at

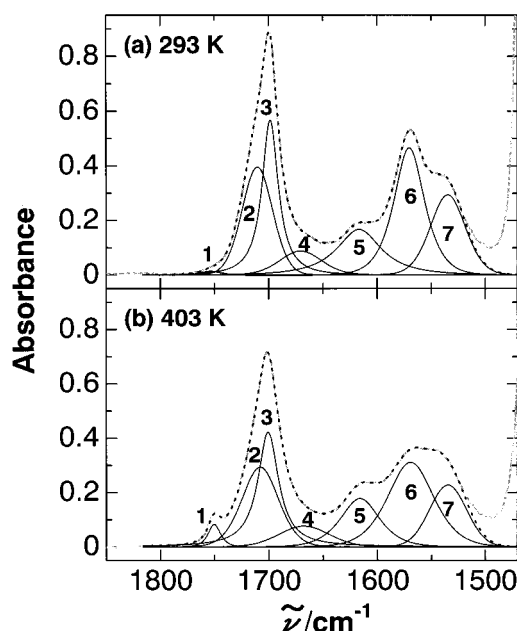


Figure 7. Computer-resolved spectra of EMAA–0.3Na/EMAA–0.6Zn (75/25 w/w) (a) at 293 K and (b) at 403 K, where thin, dotted, and solid curves are observed spectrum, the sum of seven component spectra, and component spectra, respectively. Peak positions: at 293 K, 1752.8, 1710.3, 1698.5, 1670.6, 1616.7, 1570.2, and 1534.6 cm^{-1} ; at 403 K, 1750.2, 1707.9, 1700.7, 1667.8, 1616.1, 1569.2, and 1534.6 cm^{-1} .

1750 and 1612 cm^{-1} and five minima at 1714, 1698, 1665, 1570, and 1536 cm^{-1} . Although it may be in principle possible that this region contains IR bands of constant intensities with temperature, we first started the band resolution calculation by assuming the presence of seven IR bands at the designated wavenumbers in Figure 6.

Figure 7 shows the computer-resolved spectra in the region 1800–1500 cm^{-1} for EMAA–0.3Na/EMAA–0.6Zn (75/25 w/w) at 293 K in (a) and at 403 K in (b). One can see that at both temperatures the observed pattern is well reproduced by the calculated spectrum. The fitting for other temperatures was also very satisfactory, and at all temperatures, the final root-mean-square of the residual differences between the calculated and experimental points over the range of 1796–1522 cm^{-1} was less than 3×10^{-3} in intensity units. On the other hand, the variation in wavenumber of the resolved peaks 1–7 with temperature was less than 4 cm^{-1} , which also indicates that these fittings are valid. Among the seven peaks, peaks 1–4 are associated with carbonyl $\text{C}=\text{O}$ stretching ($\nu(\text{C}=\text{O})$) vibrations. The presence of peak 4 is not apparent in the room-temperature spectrum (see Figure 4), but a similar band is observed in this region in other EMAA ionomers such as the cobalt-(II)¹⁶ or neodymium(III)¹⁷ salts, and assigned to the $\nu(\text{C}=\text{O})$ band of cyclic dimers whose oxygen is coordinated to metal cations. The same assignment is adopted to peak 4. According to Ng and Shurvell²⁵ and Tanaka et al.,²⁶ the assignment of peaks 1–3 is as follows: peak 1, free COOH ; peak 2, linear COOH dimer; peak 3, cyclic COOH dimer. Peaks 5–7 are assigned to COO^- asymmetric stretching vibrations. It is certain that peak 6 (termed the “1569 cm^{-1} band” in this paper) is assigned to (or, more strictly speaking, peak 6 contains a component of) carboxylates bridging between sodium and zinc ions. At present, the detailed assignments of peaks

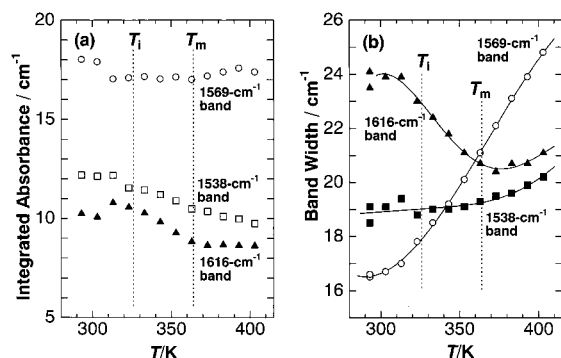


Figure 8. (a) Integrated absorbances and (b) bandwidths of three carboxylate asymmetric stretching bands as a function of temperature. T_i and T_m are peak temperatures of a transition associated with ionic aggregate region and of melting of the polyethylene crystalline region, respectively, determined by DSC.⁶

5 and 7 (termed “1616 cm^{-1} band” and “1538 cm^{-1} band”, respectively) are not clear.³⁰

Temperature Dependence of $\nu_{\text{as}}(\text{COO}^-)$ Bands.

Figure 8 shows plots of integrated absorbances and bandwidths (half-bandwidth) of three $\nu_{\text{as}}(\text{COO}^-)$ components vs temperature. In part a, the integrated absorbance of the 1616 cm^{-1} band begins to decrease at around T_i , and this decrease almost ceases at around T_m . The 1538 cm^{-1} band shows a similar temperature dependence. The magnitude of the decrease between T_i and T_m was 19% for the 1616 cm^{-1} band and 17% for the 1538 cm^{-1} band. The absorbance of the 1569 cm^{-1} band is, on the contrary, almost constant with temperature. In part b, as temperature increases, the bandwidth of the 1538 cm^{-1} band initially shows a constant value, but above T_m , it slightly increases. That of the 1616 cm^{-1} band, on the other hand, begins to decrease around T_i , but this decrease turns to a slight increase above T_m . Although the detailed assignments of these two bands are not clear, spectral changes occurring at T_i indicate that the local environments of neutralizing cations change at T_i . The notable change is seen in the 1569 cm^{-1} band. The bandwidth, which is 16.5 cm^{-1} at 293 K, begins to increase near 310 K, around T_i , and after that, increases almost linearly with temperature. This increase continues beyond T_m and up to 403 K, at which the bandwidth of the 1569 cm^{-1} band is 24.8 cm^{-1} , about a 50% increase from 293 K.

We focus attention on the temperature behavior of the 1569 cm^{-1} band. The broadening of the band with increasing temperature reflects the increased distribution of the environments of carboxylate groups bridging sodium and zinc cations with temperature. Since the carboxylate groups are attached to the polyethylene backbones, they may be sensitive to the thermal agitation of the backbones. The thermal motions of backbone are in general activated above its glass transition temperature, T_g . The T_g for polyethylene backbone is ~ 260 K, which was determined by dynamic mechanical measurements.⁶ In EMAA ionomers, however, the thermal motions are not fully activated even above T_g , because ionic aggregates and polyethylene crystalline regions still act as physical cross-links of the backbones. From Figure 5, it was concluded that the potential melting of the polyethylene crystalline region starts to occur around room temperature, and the process would promote thermal motions of the backbones. On the other hand, the fact that increased distribution occurs above

T_i suggests that above T_i the state of the bridging carboxylates is changed into the state more vulnerable to the thermal agitation from the backbones to which the carboxylate groups are attached. Therefore, the result of Figure 8 gives us the following picture on the transition at T_i . Above T_i , the ionic aggregates partly lose their ability to restrain the mobility of chain segments attached to them, and are transformed into a “disordered” state, largely subject to thermal disturbance originating from the backbones. A similar interpretation has been presented to explain the temperature behaviors of ESR spin probes intercalated into the water-swollen EMAA ionomers.³¹ The picture obtained here is quite consistent with the ionic aggregate transition model of EMAA ionomers proposed by our research group.^{7,32}

Comparison with Related Measurements. In the previous paper,⁶ it was shown that in EMAA–0.3Na/EMAA–0.6Zn (75/25 w/w) the transition at T_i on DSC is irreversible with temperature and the DSC T_i peak disappears on heating immediately after cooling from T_m but reappears on heating after aging at room temperature for at least several days from the cooling. On the contrary, as mentioned in the discussion in Figure 4, the IR spectral change in the $\nu_{\text{as}}(\text{COO}^-)$ bands was reversible with temperature. This apparent discrepancy is, however, reconciled by considering that after cooling from T_m to room temperature, the reorganization of disordered ionic aggregate region proceeds at room temperature through two relaxational processes, a faster process (F process) and a slower process (S process), as pointed out in our previous papers.^{7b,16} A reordering of the first coordination shell around metal cation would occur almost adiabatically (F process), which is detected as a reversible IR spectral change. This adiabatic change, however, would cause an imbalance between the first coordination shell and its surrounding portion, which relaxes toward a final equilibrium with much longer time, about 30 days at room temperature (S process). Therefore, the discrepancy between the IR and DSC measurements is associated with the difference in distance scale between those two measurements can detect.

Finally, it is noted that the IR $\nu_{\text{as}}(\text{COO}^-)$ bands are not always sensitive to the transition at T_i . For example, the IR spectra of EMAA–0.6Na show a broad $\nu_{\text{as}}(\text{COO}^-)$ peak at 1550 cm^{-1} at 303 K, which only sharpens a little bit when the temperature is raised to 392 K. EMAA–0.6Cu shows a sharp peak for $\nu_{\text{as}}(\text{COO}^-)$ at 1603 cm^{-1} at 303 K, and the intensity decreases only 2% with an increase in temperature to 373 K.³³ The DSC curves (10 K/min) of EMAA–0.6Na and EMAA–0.6Cu show T_i peaks at 323 and 328 K, respectively. In the two examples, the ionic nature of the $\text{COO}^- \text{Na}^+$ bond and a relatively rigid dimer structure for Cu(II) carboxylates^{34,35a} are responsible for the less prominent temperature dependence of the $\nu_{\text{as}}(\text{COO}^-)$ bands; it is theorized that the T_i transition does affect the dynamical state of cations but their local environment including symmetry around cation remains totally unchanged in both ionomers. On the other hand, the $\nu_{\text{as}}(\text{COO}^-)$ band of EMAA–0.6Co shows a remarkable change with increasing temperature, as reported previously, and this spectral change was explained by the transformation from octahedral to tetrahedral coordination in the Co(II) salts with temperature, where coordination of oxygen atoms from unneutralized COOH groups and

their detachment are responsible for the transformation.¹⁶ In other words, the IR $\nu_{\text{as}}(\text{COO}^-)$ bands can be a probe for the transition at T_i , only if the coordination structure contains a weak bond which is severely influenced by the transition. In the sodium–zinc mixed ionomers, the bridging modes of $\text{Na}^+ - \text{OCO}^- - \text{Zn}^{2+}$ would be vulnerable to the thermal agitation from the backbones, and thus the $\nu_{\text{as}}(\text{COO}^-)$ band at 1569 cm^{-1} acts as a probe monitoring the dynamics of ionic aggregates and their transition at T_i .

Blending two EMAA ionomers is a very important and attractive subject from a technological point of view. The IR studies have provided microscopic information about how the ionic aggregates are formed and how the formation results in the improvement in performance. We are now exploring other combinations of the neutralizing cations in EMAA ionomers to design the desired ionomer properties, where IR spectroscopy will be useful for the characterization, but as commented,³⁰ it is also necessary to use the aid of other experimental techniques, such as EXAFS, XANES, and ESR,^{31,35} for better understanding.

Conclusions

In the binary blends of sodium- and zinc-salt EMAA ionomers, the X-ray scattering results suggest that sodium and zinc cations are mixed at the molecular level to form ionic aggregates and that the formation is more promoted than expected for a simple mixing of EMAA–0.3Na and EMAA–0.6Zn. The IR spectra show a new asymmetric carboxylate stretching ($\nu_{\text{as}}(\text{COO}^-)$) band at 1569 cm^{-1} . This band, which is absent for individual ionomers, is assigned to carboxylate groups bridging sodium and zinc cations. In the far-IR spectra, the peak at $\sim 530\text{ cm}^{-1}$, attributable to out-of-plane COO^- bending vibrations, is substantially reduced in the sodium–zinc mixed ionomers, which also supports the above assignment of the 1569 cm^{-1} band. The 1569 cm^{-1} band acts as a probe monitoring the dynamics in the ionic aggregates with increasing temperature, and the obtained temperature dependence provides information on the transition at T_i . Above T_i , the ionic aggregates partly lose their ability to restrain the mobility of chain segments attached to them, and are transformed into the “disordered” state, largely subject to thermal disturbance originating from the backbones. This picture is consistent with our model of the ionic aggregate transition of EMAA ionomers.

Acknowledgment. We wish to thank Dr. Eisaku Hirasawa of Fujimori-Kogyo Co. for his helpful discussions. We also thank the Instrument Center, Institute of Molecular Science, Okazaki, Japan, for assistance in obtaining the X-ray scattering, and Mr. Atsushi Kato for his assistance of temperature-dependent IR measurements.

References and Notes

- (1) (a) Rees, R. W.; Vaughan, D. J. *Polym. Prepr. (Am. Chem. Soc., Div. Polym. Chem.)* **1965**, 6, 287. (b) Rees, R. W.; Vaughan, D. J. *Polym. Prepr. (Am. Chem. Soc., Div. Polym. Chem.)* **1965**, 6, 296.
- (2) *Ionic Polymers*; Holliday, L., Ed.; Applied Science: London, 1975.
- (3) *Structure and Properties of Ionomers*; Pineri, M., Eisenberg, A., Eds.; NATO ASI Series C, Mathematical and Physical Sciences; D. Reidel: Dordrecht, The Netherlands, 1987; Vol. 198.
- (4) *Ionomers: Characterization, Theory, and Applications*; Schlick, S., Ed.; CRC Press: Boca Raton, FL, 1996.
- (5) (a) Molitor, R. P. U.S. Patent 3 819 768, 1974. (b) Melvin, T. U.S. Patent 4 911 451, 1990. (c) Pocklington, T. W.; Balch, T. R. International Patent WO 92/02279, 1992.
- (6) Tachino, H.; Hara, H.; Hirasawa, E.; Kutsumizu, S.; Yano, S. *Macromolecules* **1994**, 27, 372.
- (7) (a) Tadano, K.; Hirasawa, E.; Yamamoto, Y.; Yamamoto, H.; Yano, S. *Jpn. J. Appl. Phys.* **1987**, 26, L1440. (b) Tadano, K.; Hirasawa, E.; Yamamoto, H.; Yano, S. *Macromolecules* **1989**, 22, 226. (c) Hirasawa, E.; Yamamoto, Y.; Tadano, K.; Yano, S. *Macromolecules* **1989**, 22, 2776.
- (8) Goddard, R. J.; Grady, B. P.; Cooper, S. L. *Macromolecules* **1994**, 27, 1710.
- (9) Hirasawa, E.; Yamamoto, Y.; Tadano, K.; Yano, S. *J. Appl. Polym. Sci.* **1991**, 42, 351.
- (10) Coleman, M. M.; Painter, P. C. *J. Macromol. Sci., Rev. Macromol. Chem.* **1978**, C16, 197.
- (11) Uemura, Y.; Stein, R. S.; MacKnight, W. J. *Macromolecules* **1971**, 4, 490.
- (12) (a) MacKnight, W. J.; McKenna, L. W.; Read, B. E.; Stein, R. S. *J. Phys. Chem.* **1968**, 72, 1122. (b) Earnest, T. R., Jr.; MacKnight, W. J. *Macromolecules* **1980**, 13, 844.
- (13) Brozoski, B. A.; Coleman, M. M.; Painter, P. C. *Macromolecules* **1984**, 17, 230.
- (14) Han, K.; Williams, H. L. *J. Appl. Polym. Sci.* **1989**, 38, 73.
- (15) Coleman, M. M.; Lee, J. Y.; Painter, P. C. *Macromolecules* **1990**, 23, 2339 and references therein.
- (16) Kutsumizu, S.; Kimura, H.; Mohri, F.; Hara, H.; Tachino, H.; Hirasawa, E.; Yano, S. *Macromolecules* **1996**, 29, 4324.
- (17) Kutsumizu, S.; Ikeno, T.; Osada, S.; Hara, H.; Tachino, H.; Yano, S. *Polym. J.* **1996**, 28, 299.
- (18) (a) Ishioka, T. *Polym. J.* **1993**, 25, 1147. (b) Ishioka, T.; Shimizu, M.; Watanabe, I.; Harada, M.; Kawauchi, S. *Rep. Prog. Polym. Phys. Jpn.* **1997**, 40, 447.
- (19) (a) Tsatsas, A. T.; Risen, W. M., Jr. *Chem. Phys. Lett.* **1970**, 7, 354. (b) Tsatsas, A. T.; Reed, J. W.; Risen, W. M., Jr. *J. Chem. Phys.* **1971**, 55, 3260.
- (20) Mattera, V. D., Jr.; Risen, W. M., Jr. *J. Polym. Sci., Polym. Phys. Ed.* **1984**, 22, 67.
- (21) Tsunashima, K.; Kutsumizu, S.; Hirasawa, E.; Yano, S. *Macromolecules* **1991**, 24, 5910.
- (22) Kutsumizu, S.; Hara, H.; Tachino, H.; Kato, A.; Yano, S. Presented at the 50th Yamada conference and second international symposium on polyelectrolytes, CP4–6, 31 May–3 June, 1998, Inuyama, Japan.
- (23) Minami, S. *Processing of Wave Signals for Scientific Measurements*; CQ Press: Tokyo, 1986 [in Japanese].
- (24) (a) Davidson, W. C. *AEC Research and Development Report*; AEC, Oak Ridge, TN, 1959; ANL-5990. (b) Fletcher, R.; Powell, M. J. D. *Comput. J.* **1963**, 6, 163.
- (25) Ng, J. B.; Shurvell, H. F. *J. Phys. Chem.* **1987**, 91, 496.
- (26) Tanaka, N.; Kitano, H.; Ise, N. *J. Phys. Chem.* **1990**, 94, 6290.
- (27) Davidson, A. W.; McAllister, W. H. *J. Am. Chem. Soc.* **1930**, 52, 519.
- (28) Stoilova, D.; Nikolov, G. S.; Balarev, C. *Izv. Khim.* **1976**, 9, 371.
- (29) Snyder, R. G.; Schachtschneider, J. H. *Spectrochim. Acta* **1963**, 19, 85.
- (30) In the zinc salt ionomers, Coleman et al.¹⁵ assigned two $\nu_{\text{as}}(\text{COO}^-)$ bands at 1620 and 1537 cm^{-1} to an acid salt structure around the zinc cation, and our extended X-ray absorption fine structure (EXAFS) studies have supported their assignment (as reported in Tsunashima, K.; Nishioji, H.; Hirasawa, E.; Yano, S. *Polymer* **1992**, 33, 1809). However, it is not certain whether their assignment is valid for the two bands at 1616 and 1538 cm^{-1} in a binary blend, EMAA–0.3Na/EMAA–0.6Zn (75/25 w/w), because this ionomer contains sodium cations as well as zinc cations. Moreover, very recently, Ishioka et al. proposed another interpretation in terms of the transition dipole–transition dipole interaction for the spectral change of the $\nu_{\text{as}}(\text{COO}^-)$ bands in the zinc salt ionomers with the water content, on the basis of the X-ray absorption near edge structure (XANES) experiment.¹⁸ We believe at this stage the assignment by Coleman et al. is more plausible (but this is not a subject of this paper).
- (31) (a) Kutsumizu, S.; Hara, H.; Schlick, S. *Macromolecules* **1997**, 30, 2320. (b) Kutsumizu, S.; Schlick, S. *Macromolecules* **1997**, 30, 2329.
- (32) (a) Kutsumizu, S.; Nagao, N.; Tadano, K.; Tachino, H.;

- Hirasawa, E.; Yano, S. *Macromolecules* **1992**, *25*, 6829. (b) Yano, S.; Tadano, K.; Nagao, N.; Kutsumizu, S.; Tachino, H.; Hirasawa, E. *Macromolecules* **1992**, *25*, 7168.
- (33) Kutsumizu, S.; Yano, S. Unpublished results.
- (34) Yamauchi, J.; Yano, S.; Hirasawa, E. *Makromol. Chem., Rapid. Commun.* **1989**, *10*, 109.
- (35) (a) Yamauchi, J.; Narita, H.; Kutsumizu, S.; Yano, S. *Macromol. Chem. Phys.* **1995**, *196*, 3825. (b) Yamauchi, J.; Narita, H.; Kutsumizu, S.; Yano, S. *Macromol. Chem. Phys.* **1995**, *196*, 3919.

MA9905728